

Influence of Adsorbed Water on the Oxygen Evolution Reaction on Oxides

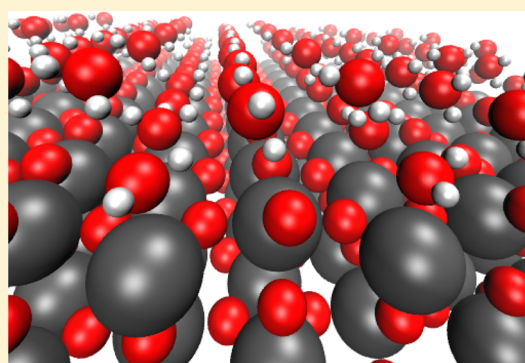
S. Siahrostami^{†,‡,§} and A. Vojvodic^{*,†,‡}

[†]SUNCAT Center for Interface Science and Catalysis, Department of Chemical Engineering, Stanford University, Stanford, California 94305, United States

[‡]SLAC National Accelerator Laboratory, 2575 Sand Hill Road, Menlo Park, California 94025, United States

[§]Center for Atomic-Scale Materials Design, Department of Physics, Technical University of Denmark, Building 307, DK-2800 Kgs. Lyngby, Denmark

ABSTRACT: We study the interface between adsorbed water and stoichiometric, defect-free (110) rutile oxide surfaces of TiO₂, RuO₂, and IrO₂ in order to understand how water influences the stabilities of the intermediates of the oxygen evolution reaction (OER). In our model the water is treated as explicitly adsorbed H₂O molecules, which are found to form two-dimensional water chains (layers) on all investigated oxide surfaces. The first chain formed by the most strongly bound H₂O molecules is adsorbed on the 5-fold coordinated surface metal atoms. The second chain is composed of less strongly bound H₂O molecules binding to bridging oxygens. The third chain interacts weakly and predominantly with the H₂O molecules of the second layer, resembling bulk water. We find that the stability of the water layer close to the oxide surface is almost the same as the one found on flat metal surfaces, such as the Pt(111) surface, despite the highly different adsorption pattern of the water molecules. We show that the presence of a water network has some effect on the interaction of individual intermediates of the OER with the oxide surface. However, the theoretical OER overpotential remains almost unchanged in the case of RuO₂ and IrO₂, while it is increased by ~0.4 eV for TiO₂.



1. INTRODUCTION

The presence of water is highly important in a large number of chemical and biological reactions. In many cases even the reaction itself relies on the presence of water. For example, the central role of water in enzymatic catalysis has long been studied.¹ Water can also act as an electrolyte in a large number of electrocatalytic reactions such as electrolysis and photolysis. For electrocatalytic and photocatalytic reactions taking place in water it is essential to include the effect of solvation of reactants, intermediates, and products at the surface.^{2–4} However, modeling water in computational studies is complex and requires very efficient functionals describing hydrogen bonding interactions; therefore, it has only been done for a limited number of surfaces.^{5–9} For example, water splitting and the two subreactions, the hydrogen evolution reaction (HER) and the oxygen evolution reaction (OER), are in most cases studied theoretically without explicitly including the water. One reason is that the molecular scale structure of adsorbed water on metal oxides is still controversial. On metal surfaces,^{5–9} water desorption is facile, while MO₂(110) oxide surfaces strongly chemisorb molecular water via interaction between the lone pair of the oxygen atom and the 5-fold coordinated metal sites, which act as acidic adsorption sites.² Even more importantly is whether the presence of water affects the OER chemistry.

Adsorption of water on TiO₂ surfaces has been widely studied both experimentally and theoretically due to the importance of aqueous–solid interfacial interaction in catalytic, electrochemical, and photochemical applications of TiO₂-based systems.^{10–19} Most of the experimental results agree that water does not dissociate on TiO₂(110), except at defect sites. While some early theoretical studies predicted dissociative H₂O adsorption,^{12,19} most of the recent studies acknowledge that water adsorbs molecularly on a stoichiometric defect-free TiO₂(110) surface and that dissociative adsorption of water only occurs on structural defects such as kinks, steps, or oxygen vacancies.^{10,15,16} A recent density functional theory (DFT) study combined with scanning tunneling microscopy (STM) measurements clarifies that there is formation of water chains on TiO₂(110).²⁰ Kimmel et al. also investigated adsorption of thin water films on the TiO₂(110) surface with ab initio molecular dynamics and infrared reflection-adsorption spectroscopy and showed an anisotropy in the water film and shed light on hydrogen bonding between water molecules in the first and second monolayers.²¹ Using ab initio molecular dynamics, Liu et al. show the presence of two distinct water layers consisting of intact water molecules in the aqueous water film

Received: September 3, 2014

Revised: December 11, 2014

Published: December 17, 2014

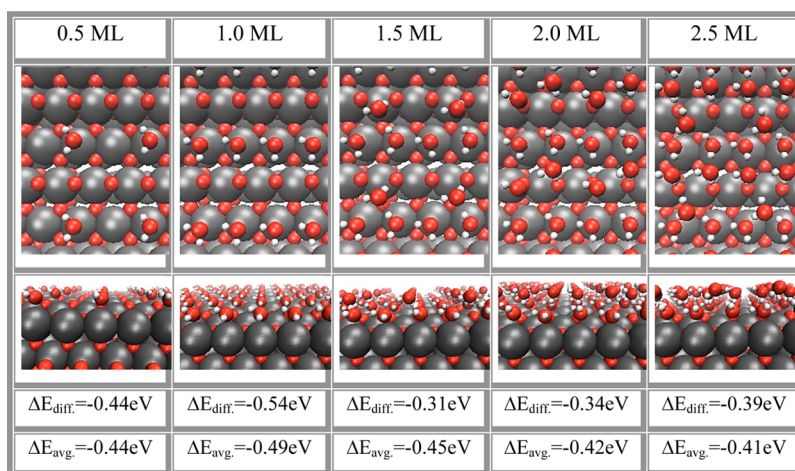


Figure 1. Top and side views of the most stable configuration for different water coverages on the defect-free $\text{TiO}_2(110)$ surface. Differential and average adsorption energies are given in the last rows. Titanium, oxygen, and hydrogen atoms are represented by dark gray, red, and white spheres. The surface is repeated several times in both the $[100]$ and $[010]$ directions.

on $\text{TiO}_2(110)$.¹⁰ They also find that independent of the exchange-correlation functional used, the first water layer comprised bound water molecules attached to the 5-fold coordinated Ti sites, while the second layer is composed of even weaker bound water molecules interacting with bridging oxygens of the $\text{TiO}_2(100)$ surface.¹⁰

Compared to numerous studies on TiO_2 , there are only a few studies on the interaction of water with other rutile transition metal oxide surfaces. Water adsorption on the $\text{RuO}_2(110)$ surface has been studied with high-resolution electron energy loss spectroscopy (HREELS) and thermal desorption spectroscopy (TDS), which found that the first water layer consists of molecularly adsorbed water on the 5-fold coordinated metal sites, while the second water layer comprises bounded water molecules on the bridging oxygen site of the $\text{RuO}_2(110)$ surface.² To the best of our knowledge there is no report on water adsorption on $\text{IrO}_2(110)$.

In this contribution, we perform a systematic DFT modeling study of adsorbed water structures on the stoichiometric defect-free rutile (110) oxide surface of TiO_2 , RuO_2 , and IrO_2 . The goals are to model the water structures on the oxide surfaces and to investigate the effect of the water network on the binding between the individual intermediates relevant for OER and the oxide surfaces by means of DFT.

2. COMPUTATIONAL DETAILS

All electronic structure calculations were performed using the grid-based projector-augmented wave (GPAW) code.²² The RPBE exchange-correlation (xc) functional was used for all of the calculations.²³ It is known that the RPBE functional underestimates the water stability due to the lack of van der Waals forces. On a Pt(111) surface, the van der Waals forces have been included to study the interaction between H_2O molecules within a water layer, and between water layers and the metal surface.²² It has been shown that each water molecule is stabilized with ~ 0.15 eV compared to the results from standard RPBE-GGA calculations.²⁴ However, previous studies on water structures on the $\text{TiO}_2(110)$ surface have shown that for an appropriately thick slab, all xc functionals essentially give the same result independent of including van der Waals forces.¹⁰ These results show that the RPBE is reasonable for the aim of the current study.

The simulations were handled using the ASE package.²⁵ Lattice constants were optimized for the bulk structures for all of the three considered oxides. The corresponding lattice constants for TiO_2 are $a = 4.70$ Å and $c = 2.95$ Å, for RuO_2 they are $a = 4.66$ Å and $c = 3.16$ Å, and for IrO_2 they are $a = 4.61$ Å and $c = 3.23$ Å. All the surfaces were modeled by a periodically repeated 2×2 unit cell in the x - and y -directions and a four layer thick slab. The two topmost layers were allowed to relax. Twenty angstroms of vacuum was used to separate successive slabs in the direction perpendicular to the surface. The Brillouin zone was sampled with a $4 \times 4 \times 1$ Monkhorst–Pack k -point grid. The geometry optimizations were carried out using the quasi-Newton minimization scheme, and the calculations were considered converged when the residual forces were smaller than 0.05 eV/Å. All calculations were performed with a grid spacing of $h = 0.18$ Å as a trade-off between computational efficiency and accuracy.

3. RESULTS AND DISCUSSION

Water adsorption on the defect-free rutile oxide (110) surface of TiO_2 , RuO_2 , and IrO_2 is studied. We investigate the coverage dependence on the adsorption properties of the water structures starting from the low coverage of 0.5 ML to coverage of 2.5 ML relative to the 5-fold surface metal atoms in the 2×2 super cell. Numerous different adsorbed water configurations have been considered. In the following subsections, we first report on the most stable water structures on the oxide surfaces that we have identified. Subsequently, we model adsorption of all OER intermediates in the presence of the water hydrogen bonded network.

3.1. Water Adsorption on the $\text{TiO}_2(110)$, $\text{RuO}_2(110)$, and $\text{IrO}_2(110)$ Surfaces. The most stable water configurations on the $\text{TiO}_2(110)$ surface for different coverages are shown in Figure 1. First water molecules (0.5 ML coverage) chemisorb via oxygen lone pairs to the 5-fold coordinated Ti sites. The resulting water adsorption energy is -0.44 eV. At 1.0 ML coverage all the 5-fold Ti sites are covered and the first full layer of water is formed. In fact, the water molecules on the 5-fold sites form a chain of water. On one hand, they orient themselves to form hydrogen bonds between each other, and on the other hand, they point toward the bridging oxygen atoms. The adsorption energy of the second water molecule,

which completes the first water chain, is -0.54 eV, i.e., it forms a stronger bond with the surface originating from the additional hydrogen bonding and the resulting symmetric structure. The favorable formation of water chain from 0.5 to 1.0 ML is in agreement with previous reported trend of water chain formation on TiO_2 .²⁰ For the 1.5 ML coverage, the additional water molecule binds with -0.31 eV to the bridging oxygen via hydrogen bonding, as well as to the water molecules of the first water chain adsorbed on the 5-fold metal site. At 2.0 ML coverage, the second water layer is complete, forming another chain of water molecules that interacts with bridging oxygen atoms. Adsorption of this water molecule leads to reorientation of the previously adsorbed water molecules (Figure 1). The adsorption energy (-0.34 eV) is slightly stronger than the previous one. Further addition of water, i.e., 2.5 ML coverage, starts the formation of a third water layer. The adsorption energy and structure of this water molecule are shown in Figure 1. The average adsorption energy for the different considered water coverages varies from -0.41 eV to -0.49 eV, as reported in Figure 1.

Hence, our findings show that water adsorbs molecularly on the defect-free $\text{TiO}_2(110)$ surface, which is in agreement with previously reported temperature programmed desorption (TPD)³ experiments and DFT calculations.¹⁵ In addition, our data clarify that the adsorbed water molecules form different chains of water on the surface, which is in agreement with reported STM²⁰ and infrared reflection-adsorption spectroscopy²¹ experiments together with DFT²⁰ and ab initio molecular dynamic^{10,21} studies.

When it comes to the stoichiometric defect-free $\text{RuO}_2(110)$ and $\text{IrO}_2(110)$ surfaces, we find that at low coverages, 0.5 and 1.0 ML, water adsorbs strongly with -0.8 and -1.40 eV on RuO_2 and IrO_2 , respectively. In fact, at these coverages water tends to dissociate on RuO_2 and IrO_2 and hydrogenate the bridging surface oxygen atoms. Our calculations show that, at water coverages lower than 1.5 ML on the $\text{IrO}_2(110)$ surface, adsorbed water on the CUS site is activated and that it dissociates spontaneously resulting in an OH group at the CUS site and a hydroxylated bridging oxygen. At low coverages on the $\text{RuO}_2(110)$ surface, the water is less activated than the one on $\text{IrO}_2(110)$; however, the dissociation barrier is only 0.13 eV. This shows that water dissociation is facile on the $\text{RuO}_2(110)$ surface at coverages lower than 1.5 ML. Thus, considering the surfaces as hydroxylated at these coverages is a necessity. At 0.5 and 1.0 ML coverages, water adsorbs weaker and molecularly on the hydroxylated surfaces of RuO_2 and IrO_2 (-0.6 and -0.7 eV for RuO_2 and IrO_2 , respectively) as compared to the unhydroxylated surfaces.

At higher coverages than 1.0 ML, the adsorbed water on RuO_2 and IrO_2 surfaces shows similar molecular adsorption behavior as on the TiO_2 surface with formation of three distinct water chains. Therefore, at higher coverages we only include the unhydroxylated surfaces.

We find that the differential adsorption energy converges to a value of -0.3 eV for all three studied oxides. This energy is significantly smaller than the free energy of a water molecule in bulk (-0.67 eV), i.e., the energy released after bringing one water molecule from gas phase to liquid phase at room temperature. There are different reported water structures on metal surfaces^{26–36} that we would like to compare to our findings of adsorbed water on oxide surfaces. The honeycomb water structure on the $\text{Pt}(111)$ surface, for example, is composed of water molecules that are bound by -0.4 eV,

according to our DFT calculations. Hence, a water molecule in a bulk water film (given by the 2.5 ML results in Figure 2)

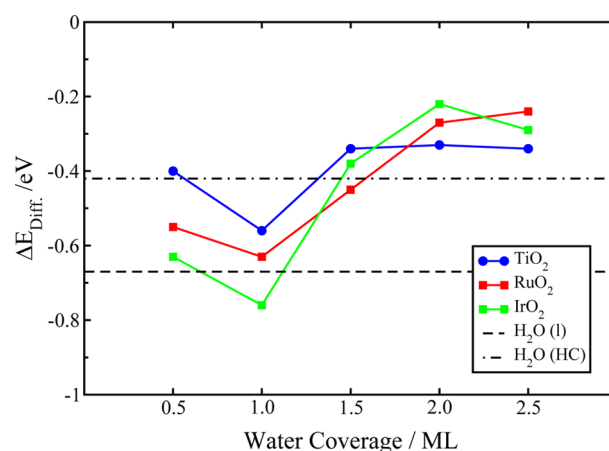
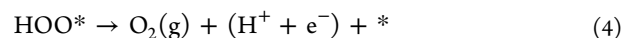
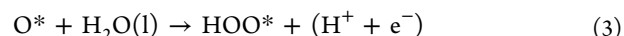
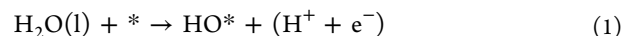


Figure 2. Calculated differential adsorption energies for the most stable water structures on oxide surface as a function of different adsorbate coverage (defined in Figure 1). The horizontal dashed-dotted line indicates the calculated binding energy of one water molecule in the honeycomb structure. The dashed horizontal line indicates the free energy of a water molecule in bulk water at room temperature.

adsorbed on the oxide surfaces is comparable to the one in a honeycomb structure on $\text{Pt}(111)$. In other words, our findings show that the adsorbed water on oxide surfaces has a completely different adsorption pattern than the one found on metal surfaces such as $\text{Pt}(111)$;^{7,26–29} however, the stability of the adsorbed water films are comparable.

3.2. Effects of Adsorbed Water on the Oxygen Evolution Reaction. The oxygen evolution reaction (OER) proceeds via a four-electron transfer with three different intermediates, i.e., HO^* , O^* , and HOO^* , as follows:



where the asterisk refers to an active site on the catalyst surface. The electrocatalytic activity is determined by the binding energies of the reaction intermediates to the electrocatalyst surface [see ref 37 for a detailed derivation]. In the following, we study the influence of adsorbed water on the individual intermediates of OER and its consequence on the overpotential of the overall reaction. We only consider the symmetric adsorbed water structures as a starting point, i.e., 1.0 and 2.0 ML coverages corresponding to complete water chains on all oxide surfaces under investigation. In all calculations, each of the OER intermediates is adsorbed on the 5-fold metal site (resulting in a coverage of 0.5 ML) and is coadsorbed with different amounts of water molecules in the above determined structures. Figure 3 displays adsorption energies of the OER intermediates, i.e., HO^* , O^* , and HOO^* as a function of total coverage, i.e., adsorbate coverage plus water coverage. We find that there are slight differences in the adsorption energies at different water coverages.

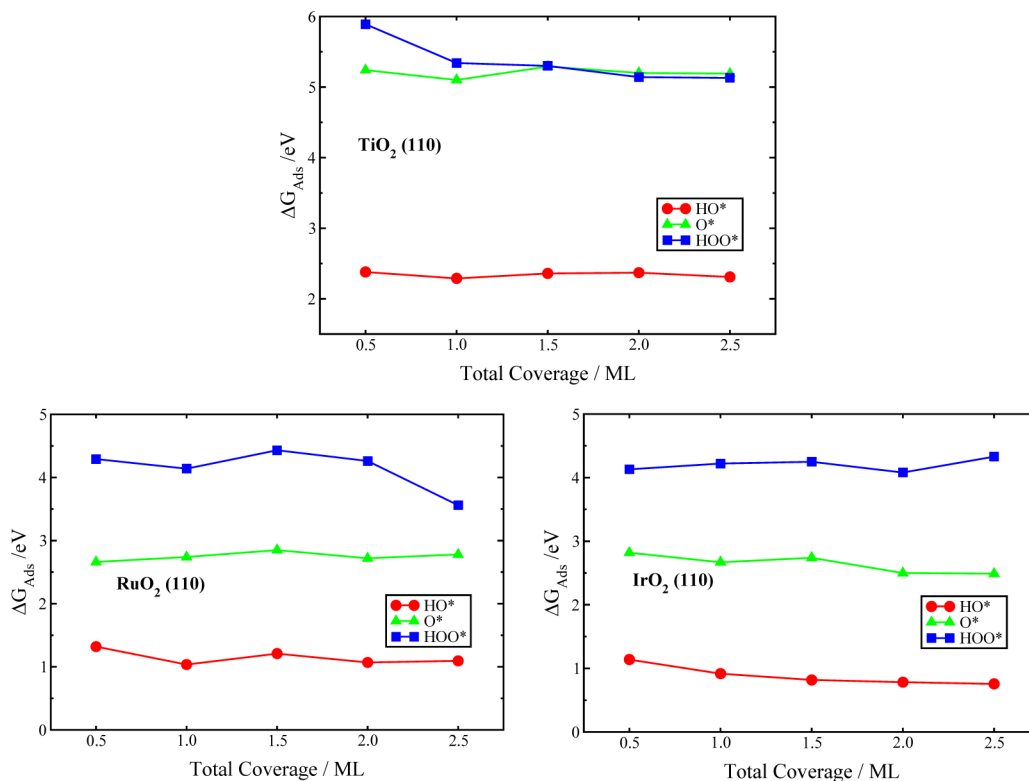
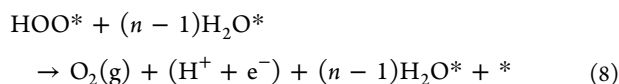
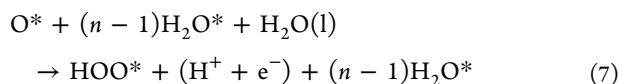
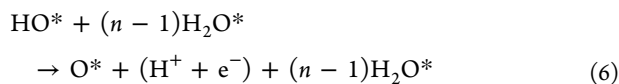
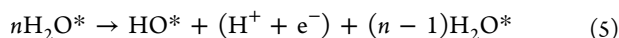


Figure 3. Calculated free energy for OER intermediates as a function of total coverage, i.e., adsorbate coverage plus water coverage, for the three studied defect-free oxide surfaces.

There are different suggested schemes that can be considered to calculate the adsorption energies of the adsorbed OER intermediates on the surface in the presence of adsorbed water.²⁴ A common feature of these schemes is that the same electron–proton transfer source is used for both the adsorbed water and for the adsorbed OER intermediates. However, for surfaces where very different adsorbed H₂O molecules coexist as we found on the (110) surfaces of rutile oxides, one should consider another scheme, given by the following equations:



This scheme involves different electron–proton transfer sources depending on the subreaction. Since the adsorbed H₂O molecules of the first chain are strongly bound to the surface, one can assume that the first and second electron–proton couple will originate from the adsorbed water chain rather than the bulk water. Hence, in the subreactions given by eqs 5 and 6, the 1.0 ML adsorbed water on the surface (Figure 1) is used as the reference. For the consecutive electron–proton transfer (eq 7), which involves formation of HOO*, we

find that the adsorbed H₂O from the second water chain (2.0 ML, Figure 1) is in equilibrium with bulk water. Therefore, we use the bulk water as reference for the subreaction given by eq 7. This assumes that the water exchange between the weakly adsorbed H₂O and the bulk water is fast, which is plausible since the energies of these water molecules are similar as discussed above. Thus, H₂O(l) in eqs 7 and 9 is the bulk water. This approach becomes rational if we include the free energy of adsorbed water ($n\text{H}_2\text{O}^*$) in the free energy diagram (FED) to account for the different references.

The calculated FEDs for OER on the TiO₂(110), RuO₂(110), and IrO₂(110) surfaces are shown in Figures 4–6, respectively. At $U = 0$ V, the largest free energy difference

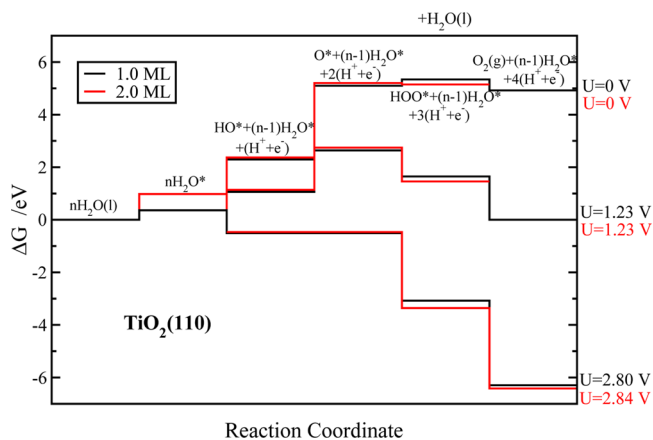


Figure 4. Calculated free energy diagram for OER on the defect-free TiO₂(110) surface covered with 1.0 ML (black) and 2.0 ML (red) water using the new scheme given by eqs 5–9

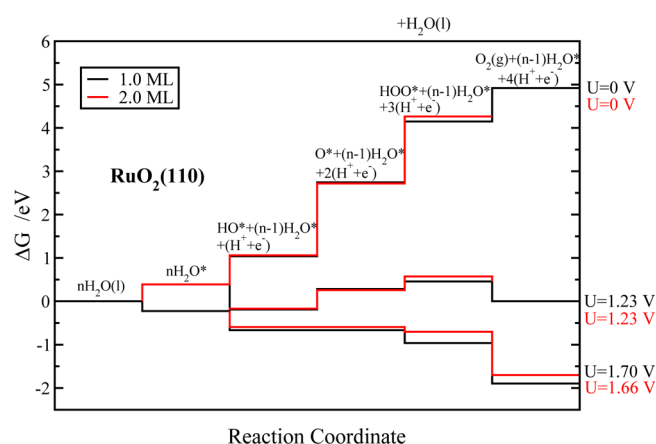


Figure 5. Same as that in Figure 4 but for the $\text{RuO}_2(110)$ surface.

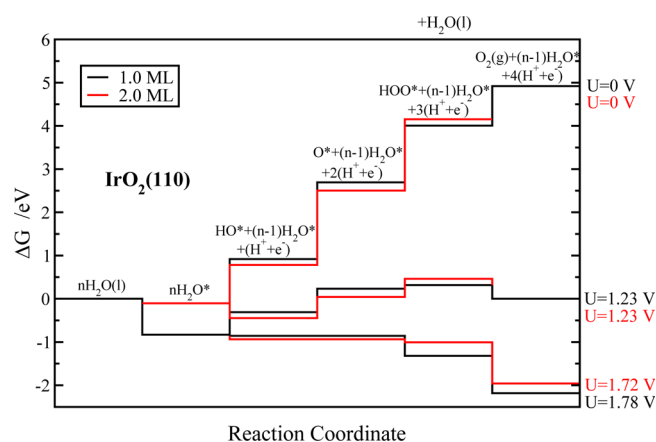


Figure 6. Same as that in Figure 4 but for the $\text{IrO}_2(110)$ surface.

between subsequent reaction steps determines the overpotential for the whole OER reaction.³⁸ For all three surfaces at both considered coverages (1.0 and 2.0 ML), we find that formation of O^* (eq 6) is the potential determining step. In addition, the overpotentials at different water coverages are found to be very similar for each individual oxide. This indicates that, even as low as one water chain, coverage should be enough to capture the electrostatic contributions from the water.

For the $\text{TiO}_2(110)$ surface the overpotentials are found to be 1.57 and 1.61 V at water coverages of 1.0 and 2.0 ML, respectively (Figure 4). Comparing these results with previously reported DFT calculations (1.19 V)³⁷ on TiO_2 shows that the OER overpotential increases by ~ 0.4 V in the presence of coadsorbed water. For the $\text{RuO}_2(110)$ surface the overpotentials are found to be 0.47 and 0.43 V at coverages of 1.0 and 2.0 ML, respectively. This is an increase of 0.1 V compared to previously reported overpotentials obtained for models without coadsorbed water (0.37 V).^{37,38} Finally, for the $\text{IrO}_2(110)$ surface, 0.55 and 0.49 V overpotentials are calculated at coverages of 1.0 and 2.0 ML, respectively. These overpotentials are on the same order as previously reported overpotential values, i.e., 0.56 V for IrO_2 , in the absence of water.^{37,39}

We find that the theoretical OER overpotentials, based on a model that explicitly includes the water network, follows the trend $\text{TiO}_2 > \text{IrO}_2 > \text{RuO}_2$. It should be stressed that this is the same order as the one found in the absence of the water

network. For all three oxide surfaces, the potential determining step changes from formation of HOO^* , without adsorbed water, to formation of O^* in the presence of water. This can be understood in terms of the stability arising due to the interaction between the coadsorbed OER intermediate and the water. Let us consider the 1.0 ML H_2O coverage as the starting point. According to the suggested mechanism (eqs 5–9), the next step is removal of one proton from one of the adsorbed water molecules to form HO^* (eq 6). This results in a very stable layer consisting of equal amounts of HO^* and H_2O , which is more strongly interacting than a full water layer.²⁴ The consecutive step (eq 7) involves removal of one more proton from this stable layer, which destroys the strong interactions between HO^* and the surrounding water molecules. Thus, we attribute the change in the potential determining step to the fact that the step corresponding to the formation of O^* requires destruction of the hydrogen bonding between HO^* and the surrounding water molecules, which costs a lot of energy.

4. CONCLUSIONS

In this work, we have systematically studied and identified the most stable adsorbed water structures at different water coverages on $\text{TiO}_2(110)$, $\text{RuO}_2(110)$, and $\text{IrO}_2(110)$ rutile oxide surfaces. We find that water forms three well-defined chains on all three studied oxides. Strongly bound water molecules form the first chain covering all the metal 5-fold sites (1.0 ML of H_2O coverage). The second water chain (2.0 ML of H_2O coverage) consists of significantly more loosely bound water, and already at this coverage the water film resembles the bulk water network. At higher water coverages a third chain of water is formed. These water films do affect the interaction between each individual OER intermediate and the oxide surfaces, in such a way that both the potential determining step changes as well as the overpotential. We have found that the presence of water only has a minor effect on the OER overpotential in the case of $\text{RuO}_2(110)$ and $\text{IrO}_2(110)$, while it increases the one for $\text{TiO}_2(110)$ by ~ 0.4 V. This implies that the OER activity trend is preserved in the presence of a water network.

AUTHOR INFORMATION

Notes

The authors declare no competing financial interest.

ACKNOWLEDGMENTS

The authors acknowledge support from the Center of Nanostructuring for Efficient Energy Conversion (CNEEC) at Stanford University, an Energy Frontier Research Center funded by the U.S. Department of Energy, Office of Basic Energy Sciences under award number DE-SC0001060. Support from the U.S. Department of Energy Office of Basic Science to the SUNCAT Center for Interface Science and Catalysis is gratefully acknowledged. S.S. acknowledges support from the Catalysis for Sustainable Energy initiative funded by the Danish Ministry of Science, Technology and Innovation, and from the Danish Council for Strategic Research's Program Commission on Strategic Growth Technologies (NABIIT). In addition, the authors acknowledge support from the Danish Center for Scientific Computing through grant HDW-1103-06. The authors are thankful for valuable discussions with Jens K. Nørskov and Jan Rossmeisl.

REFERENCES

- (1) Montiel, C.; Bustos-Jaimes, I.; Bárzana, E. Enzyme-catalyzed synthesis of heptyl- β -glycosides: effect of water coalescence at high temperature. *Bioresource Technol.* **2013**, *144*, 135–140.
- (2) Lobo, A.; Conrad, H. Interaction of H₂O with the RuO₂(110) surface studied by HREELS and TDS. *Surf. Sci.* **2003**, *523*, 279–286.
- (3) Henderson, M. A. An HREELS and TPD study of water on TiO₂(110): the extent of molecular versus dissociative adsorption. *Surf. Sci.* **1996**, *355*, 151–166.
- (4) Henderson, M. The interaction of water with solid surfaces: fundamental aspects revisited. *Surf. Sci. Rep.* **2002**, *46*, 1–308.
- (5) Ogasawara, H.; Brena, B.; Nordlund, D.; Nyberg, M.; Pelmenschikov, A.; Pettersson, L.; Nilsson, A. Structure and Bonding of Water on Pt(111). *Phys. Rev. Lett.* **2002**, *89*, 276102.
- (6) Michaelides, A.; Hu, P. A density functional theory study of hydroxyl and the intermediate in the water formation reaction on Pt. *J. Chem. Phys.* **2001**, *114*, 513.
- (7) Feibelman, P. J. Partial dissociation of water on Ru(0001). *Science* **2002**, *295*, 99–102.
- (8) Schnur, S.; Groß, A. Properties of metal–water interfaces studied from first principles. *New J. Phys.* **2009**, *11*, 125003.
- (9) Lin, X.; Groß, A. First-principles study of the water structure on flat and stepped gold surfaces. *Surf. Sci.* **2012**, *606*, 886–891.
- (10) Liu, L.-M.; Zhang, C.; Thornton, G.; Michaelides, A. Structure and dynamics of liquid water on rutile TiO₂(110). *Phys. Rev.* **2010**, *82*, 161415.
- (11) Diebold, U. The surface science of titanium dioxide. *Surf. Sci. Rep.* **2003**, *48*, 53–229.
- (12) Lindan, P. J. D.; Harrison, N. M.; Holender, J. M.; Gillan, M. J. First-principles molecular dynamics simulation of water dissociation on TiO₂(110). *Chem. Phys. Lett.* **1996**, *261*, 246–252.
- (13) Maksymovych, P.; Mezheny, S.; Yates, J. T. STM study of water adsorption on the TiO₂(110)-(1 × 2) surface. *Chem. Phys. Lett.* **2003**, *382*, 270–276.
- (14) Zehr, R. T.; Henderson, M. a. Influence of O₂-induced surface roughening on the chemistry of water on TiO₂(110). *Surf. Sci.* **2008**, *602*, 1507–1516.
- (15) Hammer, B.; Wendt, S.; Besenbacher, F. Water Adsorption on TiO₂. *Top. Catal.* **2010**, *53*, 423–430.
- (16) Sun, C.; Liu, L.-M.; Selloni, A.; Lu, G. Q. (Max); Smith, S. C. Titania-water interactions: a review of theoretical studies. *J. Mater. Chem.* **2010**, *20*, 10319.
- (17) Shen, M.; Henderson, M. A. Role of Water in Methanol Photochemistry on Rutile TiO₂(110). *J. Phys. Chem. C* **2012**, *116*, 18788–18795.
- (18) Schaub, R.; Thostrup, P.; Lopez, N.; Lægsgaard, E.; Stensgaard, I.; Nørskov, J.; Besenbacher, F. Oxygen vacancies as active sites for water dissociation on rutile TiO₂(110). *Phys. Rev. Lett.* **2001**, *87*, 266104.
- (19) Lindan, P. J. D.; Harrison, N. M. Mixed dissociative and molecular adsorption of water on the rutile (110) surface. *Phys. Rev. Lett.* **1998**, *80*, 762–765.
- (20) Lee, J.; Sorescu, D. C.; Deng, X.; Jordan, K. D. Water Chain Formation on TiO₂(110). *Phys. Rev. Lett.* **2013**, *4*, 53–57.
- (21) Kimmel, G. A.; Baer, M.; Petrik, N. G.; VandeVondele, J.; Rousseau, R.; Mundy, C. J. Polarization- and azimuth-resolved infrared spectroscopy of water on TiO₂(110): anisotropy and the hydrogen-bonding network. *J. Phys. Chem. Lett.* **2012**, *3*, 778–784.
- (22) Mortensen, J.; Hansen, L.; Jacobsen, K. Real-space grid implementation of the projector augmented wave method. *Phys. Rev. B* **2005**, *71*, 035109.
- (23) Hammer, B.; Hansen, L.; Nørskov, J. Improved adsorption energetics within density-functional theory using revised Perdew-Burke-Ernzerhof functionals. *Phys. Rev. B* **1999**, *59*, 7413–7421.
- (24) Tripkovic, V.; Skúlason, E.; Siahrostami, S.; Nørskov, J. K.; Rossmeisl, J. The oxygen reduction reaction mechanism on {Pt}(111) from density functional theory calculations. *Electrochim. Acta* **2010**, *55*, 7975–7981.
- (25) *Atomic Simulation Environment (ASE)*; Center for Atomic Scale Material Design (CAMD), Technical University of Denmark: Lyngby, Denmark; <https://wiki.fysik.dtu.dk/ase>.
- (26) Nie, S.; Feibelman, P. J.; Bartelt, N. C.; Thürmer, K. Pentagons and heptagons in the first water layer on Pt(111). *Phys. Rev. Lett.* **2010**, *105*, 026102.
- (27) Carrasco, J.; Hodgson, A.; Michaelides, A. A molecular perspective of water at metal interfaces. *Nat. Mater.* **2012**, *11*, 667–674.
- (28) Glebov, A.; Graham, A. P.; Menzel, A.; Toennies, J. P. Orientational ordering of two-dimensional ice on Pt(111). *J. Chem. Phys.* **1997**, *106*, 9382.
- (29) Standop, S.; Redinger, A.; Morgenstern, M.; Michely, T.; Busse, C. Molecular structure of the H₂O wetting layer on Pt(111). *Phys. Rev. B* **2010**, *82*, 161412.
- (30) Feibelman, P. J.; Bartelt, N. C.; Nie, S.; Thürmer, K. Interpretation of high-resolution images of the best-bound wetting layers on Pt(111). *J. Chem. Phys.* **2010**, *133*, 154703.
- (31) Forster, M.; Raval, R.; Carrasco, J.; Michaelides, A.; Hodgson, A. Water-hydroxyl phases on an open metal surface: breaking the ice rules. *Chem. Sci.* **2012**, *3*, 93.
- (32) Gawronski, H.; Carrasco, J.; Michaelides, A.; Morgenstern, K. Manipulation and control of hydrogen bond dynamics in absorbed ice nanoclusters. *Phys. Rev. Lett.* **2008**, *101*, 136102.
- (33) Mehlhorn, M.; Carrasco, J.; Michaelides, A.; Morgenstern, K. Local investigation of femtosecond laser induced dynamics of water nanoclusters on Cu(111). *Phys. Rev. Lett.* **2009**, *103*, 026101.
- (34) Morgenstern, K. Scanning tunnelling microscopy investigation of water in submonolayer coverage on Ag(111). *Surf. Sci.* **2002**, *504*, 293–300.
- (35) Morgenstern, K.; Nieminen, J. Intermolecular Bond Length of Ice on Ag(111). *Phys. Rev. Lett.* **2002**, *88*, 066102.
- (36) Mitsui, T.; Rose, M. K.; Fomin, E.; Ogletree, D. F.; Salmeron, M. Water diffusion and clustering on Pd(111). *Science* **2002**, *297*, 1850–1852.
- (37) Rossmeisl, J.; Qu, Z.-W.; Zhu, H.; Kroes, G.-J.; Nørskov, J. K. Electrolysis of water on oxide surfaces. *J. Electroanal. Chem.* **2007**, *607*, 83–89.
- (38) Nørskov, J. K.; Rossmeisl, J.; Logadottir, A.; Lindqvist, L.; Kitchin, J. R.; Bligaard, T.; Jónsson, H. Origin of the overpotential for oxygen reduction at a fuel-cell cathode. *J. Phys. Chem. B* **2004**, *108*, 17886–17892.
- (39) Man, I. C.; Su, H.-Y.; Calle-Vallejo, F.; Hansen, H. A.; Martínez, J. I.; Inoglu, N. G.; Kitchin, J.; Jaramillo, T. F.; Nørskov, J. K.; Rossmeisl, J. Universality in oxygen evolution electrocatalysis on oxide surfaces. *ChemCatChem* **2011**, *3*, 1159–1165.